A Simulation of Secondary Proton Production in ^{12}C + ^{12}C Reaction Studies

Senior Honours Project

The carbon-burning process is an important part of stellar nucleosynthesis – to better understand it, the ^{12}C (^{12}C, p) ^{23}Na and ^{12}C (^{12}C, α) ^{20}Ne fusion reactions are studied at stellar energies. A highly unlikely two-step process, due to hydrogen and deuterium contamination at levels of 0.3ppm and 0.005ppb respectively is capable of producing background radiation at the energies of interest. This makes direct measurement of these reactions difficult. Here, the results of a computational simulation aimed at modelling the three main beam-induced background reactions, the ^{12}C (d, p) ^{13}C, ^{12}C (d, d) ^{12}C, and ^{12}C (p, p) ^{12}C reactions, are reported. The simulation validates its results by producing background peaks in line with observed spectra for both Rutherford scattering reactions, and produces promising indications in preliminary fusion simulations.

Jake Watson

Supervisor: Dr. Marialuisa Aliotta

1 TABLE OF CONTENTS

Acknowledgements

I would like to thank my supervisor, Dr. Marialuisa Aliotta, for her valuable and constructive guidance in all areas of this project, and Carlo Bruno, whose extensive knowledge of C++ and willingness to give his time generously proved a great help.

2 INTRODUCTION

2.1 MOTIVATION AND AIMS

The carbon-burning process is one of several processes studied in the field of stellar nucleosynthesis – the means by which large stars gradually produce progressively heavier nuclei through fusion reactions.

The CIRCE accelerator, based in Caserta, Italy, is being used to study the reactions involved in carbon-burning. The setup of this experiment, and a detailed description of the theory, will be described in Section 3, but involves, in brief, accelerating a beam of ^{12}C nuclei towards a highly pure carbon target.

The beam nuclei interact with the target nuclei, and several reactions channels are open. Measuring the reaction products directly in this manner is difficult, as the beam also induces substantial background radiation, through a two-step process due to contaminants within the target.

This project aims to computationally simulate the beam-induced background produced by the reactions on the contaminants, so as to isolate the products of the reactions of interest.

To do this, it had to fulfil the following aims:

- Simulation of the Rutherford scattering of secondary protons and deuterons, produced through interactions of a ^{12}C beam with a ^{12}C target, by ^{12}C nuclei within the target.
- Simulation of the Rutherford scattering of secondary protons and deuterons, produced through interactions of a ^{12}C beam with a ^{12}C target, by contaminants within the target.
- Simulation of the scattering through fusion processes of secondary deuterons, produced through interactions of a ^{12}C beam with a ^{12}C target, by ^{12}C atoms within the target.

2.2 METHODS

The program used to simulate this background radiation was designed specifically for the project, and was written in C++, making use of its extensive scientific and mathematical libraries. Where possible and knowledge allowed, it was designed to increase the speed of computation. It focuses on two types of scattering: elastic Rutherford scattering, and inelastic fusion.

To simulate the passage of a beam nucleus through the target, the following steps are taken

1. The target is split up into layers, representing a single chance of interaction, such as a target atom.
2. The program calculates the energy of an ejectile induced by the carbon beam through interaction with a target contaminant.
3. It then calculates and integrates the reaction cross-section between the ejectile and the layer, and tests for interaction using a random number generator. If it interacts, it finds the scattering angle of the second ejectile
4. Finally, it finds the scattering energy of a secondary ejectile induced by the interaction of the first ejectile with a second target nucleus.

The simulated data is then compared to measured data from the CIRCE experiment, both to validate the simulation results and to find the position of peaks in the background radiation.

3 THEORY AND EXPERIMENTAL SET-UP

In this section, the design of the CIRCE experiment will be outlined, followed by an evaluation of the relevant theory.

3.1 THE CIRCE EXPERIMENT

The experiment, based at the Centre for Isotopic Research on the Cultural and Environmental heritage (CIRCE) laboratory in Caserta, aims to measure the ^{12}C (^{12}C, α) ^{20}Ne and ^{12}C (^{12}C, p) ^{23}Na reactions, which play key role during the carbon burning phase of stars. These two fusion reactions are studied by accelerating a high intensity (20 - 30 µA) beam of 2^+ carbon ions, using the 3MV pelletron tandem accelerator, towards a highly pure carbon target, composed of HOPG (Highly Ordered Pyrolytic Graphite) graphite. The target has a thickness of 2mm, and is cooled to avoid target heating and deterioration. The products of the reaction, protons from the ^{12}C (^{12}C, p) ^{23}Na reaction as well as alpha particles from the ^{12}C (^{12}C, α) ^{20}Ne, are detected at backwards angles using an array of silicon detectors, whose angles are still being optimized. This simulation focused on a detector placed at 143˚relative to the beam. [1]

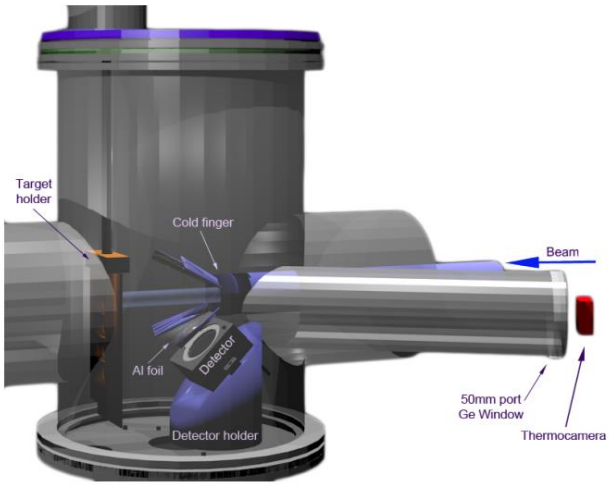

Figure 1: The CIRCE setup. This diagram lacks the second detector. [8]

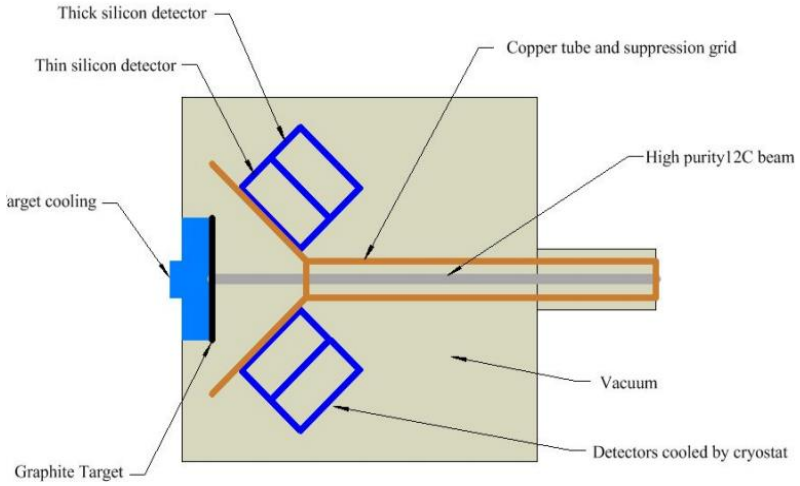

Figure 2: The detector setup, viewed from above. [9]

3.2 The "Two Step" Process

As the carbon ions interact with the target, they have several possible reactions, known as reaction channels, open to them. Along with the reaction of interest, ^{12}C (^{12}C, p) ^{23}Na, the beam nuclei could interact with the impurities within the target, mainly deuterium and hydrogen. The possible reactions in this step are shown in the 'primary' section of Table 1.

Table 1: A table of possible reactions.

Reaction	Backscatter	Interaction Type
Primary – induced directly by beam.		
^{12}C (^{12}C, p) ^{23}Na	Yes	Fusion
^{1}H (^{12}C, p) ^{12}C	No	Elastic Scattering
d (^{12}C, p) ^{13}C	Yes	Fusion
d (^{12}C, d) ^{12}C	No	Elastic Scattering
Secondary – induced by primary ejectile.		
^{12}C (p, p) ^{12}C	Yes	Elastic Scattering
^{12}C (d, d) ^{12}C	Yes	Elastic Scattering
^{12}C (d, p) ^{13}C	Yes	Fusion

The second column of Table 1 denotes whether or not that reaction can produce an ejectile at angles above 90˚ relative to the beam. As the detectors are backwards of the target (on the same side that the beam strikes), the only reactions that can contribute to the measurements are those which can backscatter.

The products of those reactions which cannot backscatter can still influence the measurements, however, through a less likely 'secondary' step. The products of these 'primary' reactions, protons and deuterons, travel through the target, until they interact with a carbon nucleus. The possible reaction channels at this point are shown in the 'secondary' section of Table 1.

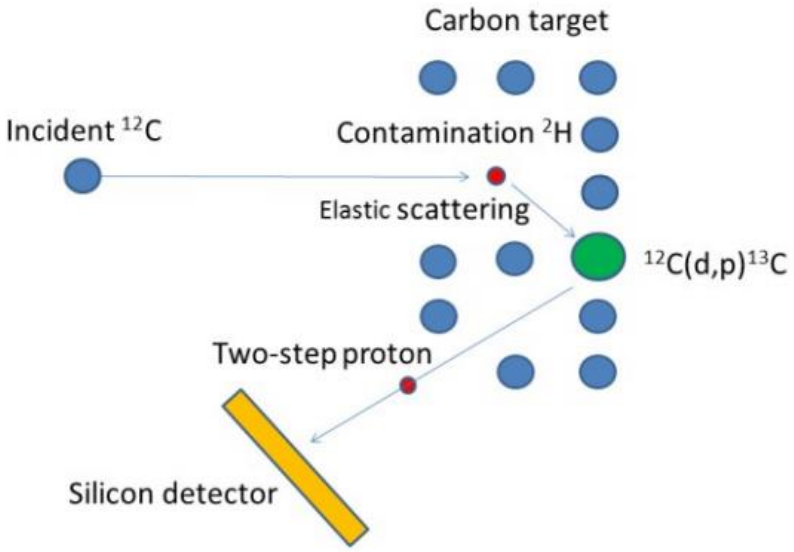

Figure 3: Schematic of the two-step process where deuterium nuclei contained within the target are elastically scattered at forward angles by incident carbon nuclei, and then interact with further target carbon nuclei. [1]

There are two means of interaction - fusion, governed by the strong force, and Rutherford scattering, governed by the electrostatic force. Each reaction is capable of producing either a proton or a deuteron at backwards angles, and can therefore contribute to the measurements.

3.2.1 Region of Interest

The energy of the carbon beam is well below the coulomb barrier for carbon fusion, so the cross-section of the ^{12}C (^{12}C, p) ^{23}Na reaction is very low. This means that the carbon-fusion signal can be easily masked by any background radiation in the energy range of these protons.

A large source of this background radiation is ambient, such as cosmic rays. To combat this, two-stage detectors are used, which eliminate much of the background through coincidence techniques and particle identification. This leaves only radiation from the target. As we have seen, there is one other reaction channel capable of producing protons at backwards angles in the 'primary' step, the d (^{12}C, p) ^{13}C fusion reaction. However, this produces protons at much lower energies than those expected for carbon fusion, and so can be easily identified and discarded.

Unfortunately, the second 'step' in the two-step process can also produce protons at backwards angles, with energies lying directly in the region of interest for carbon fusion, making these background protons hard to identify and remove. All three of the 'secondary' step reactions can backscatter, and therefore contribute to measurements. In particular, the d (^{12}C, p) ^{13}C reaction produces a significant proportion of protons in the region of interest, due to a resonance in the fusion cross-section at 1.2 MeV incident energy. This means that an incident 1.2 MeV deuteron is more likely to undergo nuclear fusion than deuterons with higher or lower energies, as shown in Figures 4 and 5.

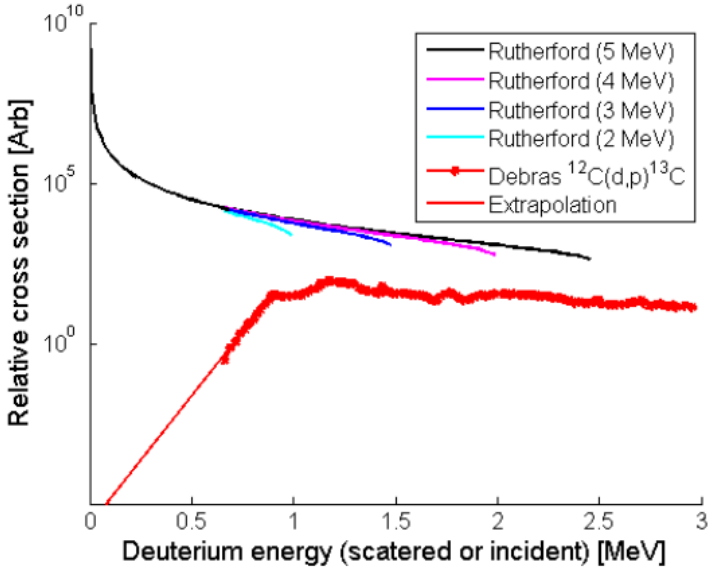

Figure 4: The smooth lines represent the Rutherford cross-section for deuterons being scattered by incident carbon nuclei at various energies, while the lower line represents the measured cross-section for the ^{12}C (d, p)^{13}C reaction and its extrapolation to low energies. [1]

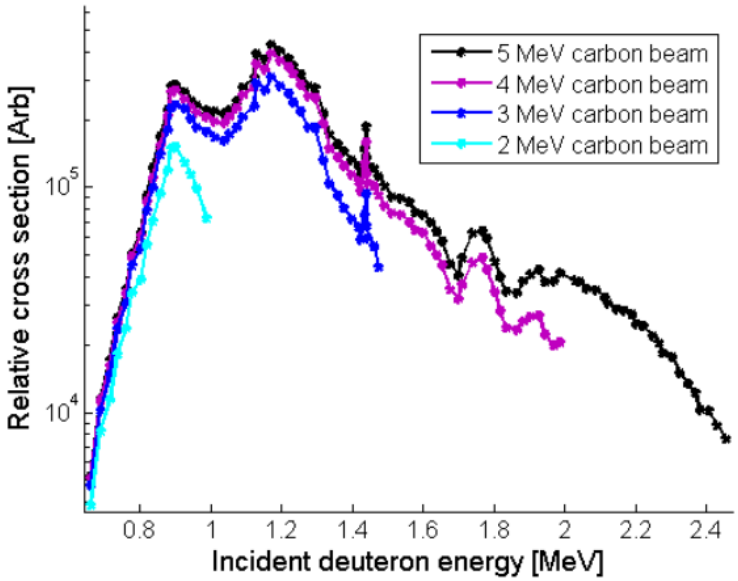

Figure 5: A detail of the fusion cross-section shown in Figure 4. The peak in cross-section shown for 1.2 MeV energy signifies a resonance.

Elastically scattered deuterons from the 'primary' step will be produced with a continuous range of energies. Normally one would expect these deuterons to produce a continuous range of ejectile protons from the 'secondary' fusion step, but this is not the case. Due to the higher probability of fusion for 1.2 MeV deuterons, the protons produced in the fusion reaction will be grouped around the resonance. These protons are produced at energies directly in the middle of the energy range of interest for the ^{12}C (^{12}C, p) ^{23}Na reaction.

3.2.2 Background Radiation Reduction

To combat this source of background, there are two choices: reduce the level of background by reducing the level of contaminants in the target, or simulate the beam-induced background and subtract this prediction from measurements.

Some of the hydrogen and deuterium contamination is due to contact with the atmosphere. However, placing the target in a vacuum did not reduce the level of background significantly, and so the target was replaced with a HOPG target, which has been shown [2] to have hydrogen contamination levels of approximately 0.3ppm, and deuterium levels of 0.005ppb. This low level of contamination is still not enough to dispel the background due to the two-step process, and so the background must be predicted. [1]

A simulation was chosen as the means of prediction. In the next section, the structure and design of the main components of the simulation are outlined.

4 METHOD

In this section, the main components and design of the simulation will be outlined, followed by an explanation of the use of the simulation. Finally, followed by an account of how it was used to obtain results will be summarized.

4.1 GENERAL CODE OUTLINE

The main steps involved in the simulation are summarized in brief in this section. A more in depth discussion of the more complex steps can be found in the next few sections.

1. To begin, the energy of the 'primary' reaction ejectile, either a proton or a neutron, must be found. Once this is done, using a straightforward elastic scattering calculation, the passage of that ejectile through the target is simulated. As an approximation, each ejectile is simulated as the 'worst kinematic case' – it has the maximum energy it is kinematically allowed to have.
2. In order to carry out this trajectory simulation, the target must be split up into layers, so that the continuous target can be discretized, and analyzed. The internal structure of the HOPG target does in fact lend itself to a layer approximation. At each of these layers, the projectile can be viewed as having a probability of interaction.
3. Now that the target has been split up into layers, the nature of such an interaction must be defined – either fusion or Rutherford scattering. For both types, the energy of the projectile is used to find a differential angular cross-section for the projectile and the layer.
4. This differential cross-section is then integrated over all angles, giving a total cross-section, and then multiplied by the target density. The result is the probability that the projectile interacts with the layer.
5. Once the particle interacts, the angle of the products must be found. To do this, the angular differential cross-section is integrated over the angular range of the detector, and then divided by the total reaction cross-section. This gives the probability that the projectile, given that it has interacted, is scattered towards the detector. It is now known as the 'secondary' ejectile.
6. Finally, using the angle of scattering, the 'secondary' ejectile's energy can be determined using a simple kinematics calculation.

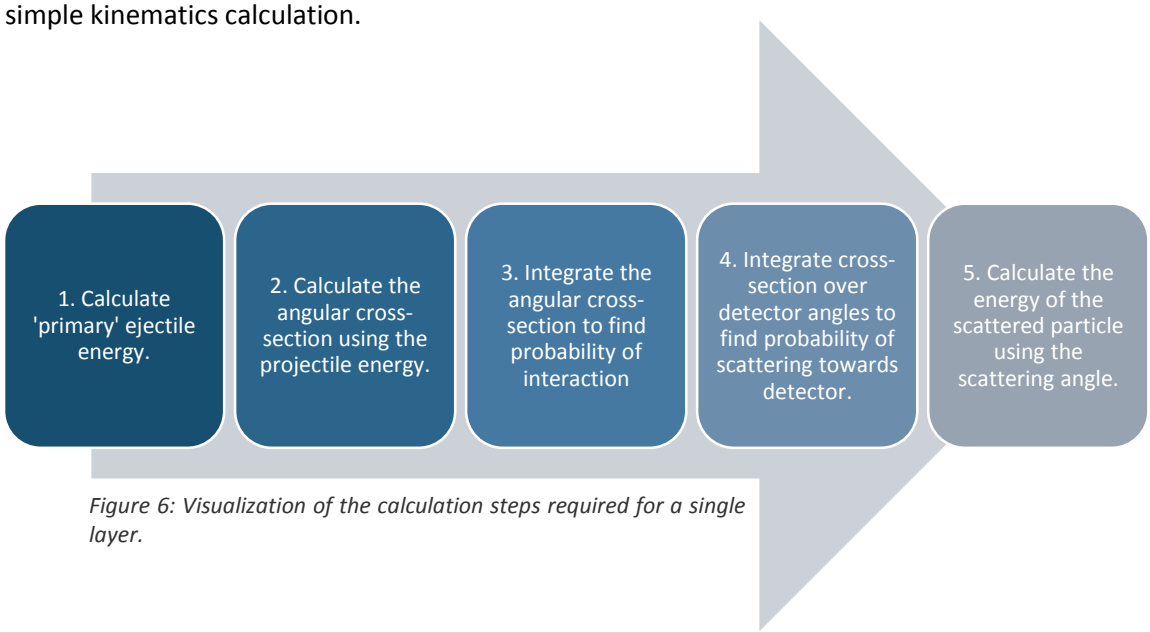

Figure 6: Visualization of the calculation steps required for a single layer.

4.2 KINEMATICS CALCULATIONS

The two types of reaction are examples of inelastic and elastic two-body scattering. In both cases the target is stationary.

4.2.1 Rutherford scattering

The energy of the ejectile from the 'primary' step is given by the following formula:

$$v_1 = \frac{2m_1u_1\cos(\theta) \pm \sqrt{4m_1^2u_1^2\cos(\theta)^2 - 4(m_1+m_2)(m_1-m_2)u_1^2}}{2(m_1+m_2)} \quad (1)$$

Where v_1 is the final velocity of the incident particle, u_1 is the initial velocity of the incident particle, m_1 is the mass of the incident particle, m_2 is the mass of the stationary target, and θ is the scattering angle of the incident particle.

This equation is also used to find the energy of the ejectile from the 'secondary' step.

4.2.2 Fusion

The fusion reaction is an example of inelastic scattering, as the reaction has a Q value of 2.7217 MeV. The energy of the ejectile from this reaction is given by:

$$\sqrt{T_3} = \frac{2\sqrt{m_1m_3T_1}\cos(\theta) \pm \sqrt{4m_1m_3T_1\cos(\theta)^2 - 4(m_3+m_4)(T_1(m_1-m_4)-m_4Q)}}{2(m_3+m_4)} \quad (2)$$

Where T_3 is the kinetic energy of the ejectile, T_1 is the kinetic energy of the projectile, m_1 is the mass of the projectile, m_1 is the mass of the projectile, m_4 is the mass of the recoil, θ is the scattering angle, and Q is the Q value for the reaction.

4.3 CALCULATING THE ANGULAR CROSS-SECTION

Both of the two types of reaction possible in the simulation, Rutherford scattering and fusion, require a different method to calculate their cross-section.

4.3.1 Rutherford Scattering

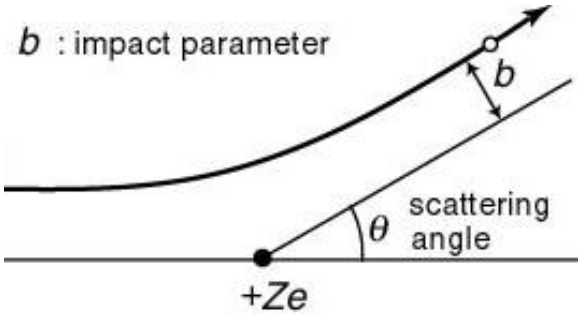

Figure 7: Sketch of Rutherford scattering.

The angular cross-section, $d\sigma/d\Omega$, for Rutherford scattering can be calculated using the following equation.

$$\frac{d\sigma}{d\Omega} = \frac{k^2Z_1^2Z_2^2e^4}{16E^2}\frac{1}{sin^4(\theta/2)} \quad (3)$$

Where Z_1, Z_2 are the nuclear charges of the reactants, $k = 1/4\pi\varepsilon_0$, e is the elementary charge, E is the kinetic energy of the projectile and ϑ is the scattering angle. The quantity dΩ represents a solid angle.

Using this formula, the simulation calculates a value for the angular cross-section in 1˚ discrete increments over a 180˚ range. A plot, Figure 8, produced by the simulation is included below. As an approximation at low angles, the cross-section at 0˚ is set to the 1˚ cross-section.

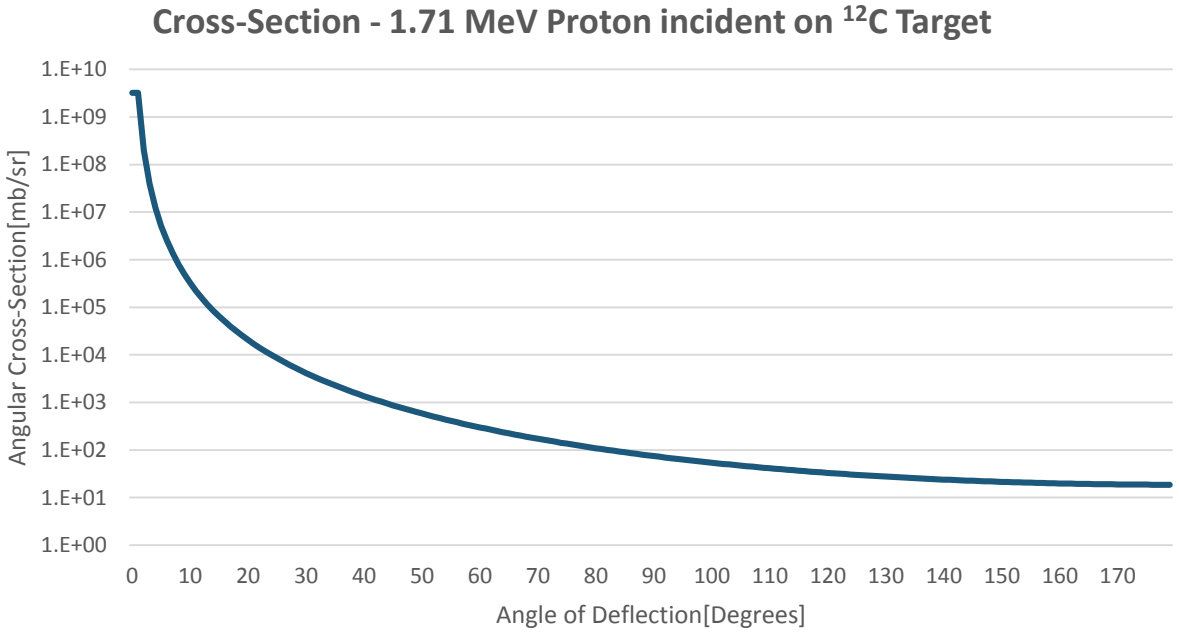

Figure 8: Calculated angular cross-section for 1.71 MeV scattered proton incident on a stationary ^{12}C nucleus.

4.3.2 Fusion

For the fusion cross-section, there is no theoretical prediction available. Therefore, measured values must be used. Lacking a full measured range of angular cross sections for several energies, a single angular differential cross-section measurement [3] shown in Figure 9 and an energy differential cross-section [4], were obtained using the EXFOR website [5]. These were used to generate approximations to the angular cross-section for various energies, although such approximations are in no way guaranteed to be close to the true value.

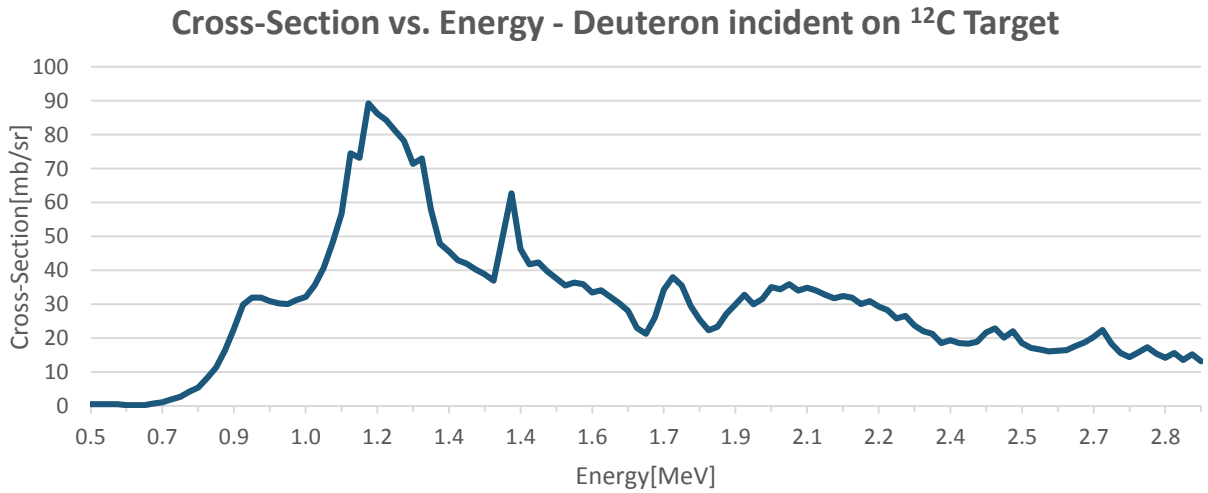

Figure 9: The energy differential cross-section obtained using the [4] data. Note the higher cross-section at 1.2 MeV, denoting a resonance. (Angle of measurement: 135˚)

4.4 Integrating the Angular Cross-Section

Once the cross-section was known, it had to be integrated, so as to find the reaction probability. Again, a different method of integration was used for each type of reaction.

4.4.1 Rutherford Scattering

An analytical integration of Eq.1 will fail, as the integral diverges. Therefore, a numerical integration method known as Monte Carlo integration was used to find the integral.

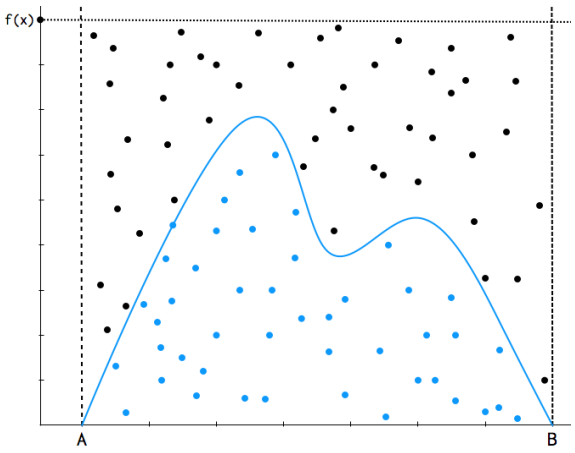

Figure 10: An illustration of the Monte Carlo numerical integration method. [10]

The steps of Monte Carlo integration are listed:

1. Place a box over the function to be integrated, with width equal to the range of integration.
2. Generate a large number of random points within this box.
3. For every point, check to see if it is greater or less than the function, for the point's x-value. The function used in this case was Eq. 3, multiplied by $2\pi\sin(\theta)$, so as to obtain the integral over all angles.
4. Count the number of points less than the function, and divide this number by the total number of points generated. This gives the fraction of the box's area occupied by the function.
5. Multiply the box's area by the fraction found in the previous step. This gives the value of the integral.

The accuracy of this method is strongly dependent upon the number of random points generated, but a very large number of points can significantly slow down the speed of the simulation.

So as to be able to determine the scattering angle, it was necessary to find the value of the integrated cross-section in 1˚ increments. To do this, the 'box' of integration for the Monte Carlo method was made to be 1˚ wide, with the integral calculated at steps of 1˚. This gave an array of integrated cross-sections for every 1˚ in a 180˚ range. For the simulation, 1000 random points were generated for every integration.

4.4.1.1 Random Number Generation

This numerical integration method, as well as several other functions throughout the code, required the use of a Pseudo-Random-Number-Generator. The C++ header file included in C++11, `<random>`, contains several random number generators based on different algorithms. In the code, the Mersenne Twister 1997 algorithm provided by `<random>` was used, as the period of the algorithm is large enough to ensure that the random number stream will not repeat, and the quality of random numbers generated is very high. To ensure that the seed of the algorithm is different every time the program is run, a high-precision system time is used.

4.4.2 Fusion

As a function for the angular distribution of the cross-section was not known, the integral was calculated using the data discussed in Section 4.3.2. For every 1˚ increment, the value of the extrapolated angular cross-section was used as the height of a rectangle, with width equal to 1˚. The area of this rectangle was found by multiplying the width and height, and multiplied by $2\pi\sin(\theta)$, so as to obtain the integral over all angles. The area of this rectangle was then taken as the integrated cross-section for that 1˚ increment,

so the total cross-section over all angles could be found by simply adding the area of every rectangle in the 180˚ range.

4.4.3 Finding the Interaction Probability

To find the total interaction probability, the cross-section was multiplied by the area density of target nuclei per layer. Assuming 1000 layers (which gives a balance between precision of the energy loss and the speed of computation), with a quoted HOPG density of 2.25g/cm^3, and using SRIM [6] to find the range of the projectile in the target, an area density of 29×10^{20} atoms/cm^2 per layer was found. In addition to this, a bias factor was used to artificially increase the integrated cross-section. For example, a bias factor of 1,000 would mean that a result of 100 protons arriving at the detector out of 1,000,000 beam particles is actually 100,000 protons arriving for every 1,000,000,000 beam projectiles.

4.5 Detector Response

The energies for the 'secondary' step ejectiles are calculated by the detector. However, these are subject to the detector response function. As the particles travel through the detector, they may interact with the detector nuclei, losing or gaining energy. Other factors intrinsic to the detector, such as electrical noise, also contribute to the change in energy or reading of the energy. This is simulated by distributing the scattered energies over a normal distribution, with mean equal to the energy of the particle, and standard deviation equal to 40 KeV [7], or the detector resolution.

4.6 Simulating Energy Loss

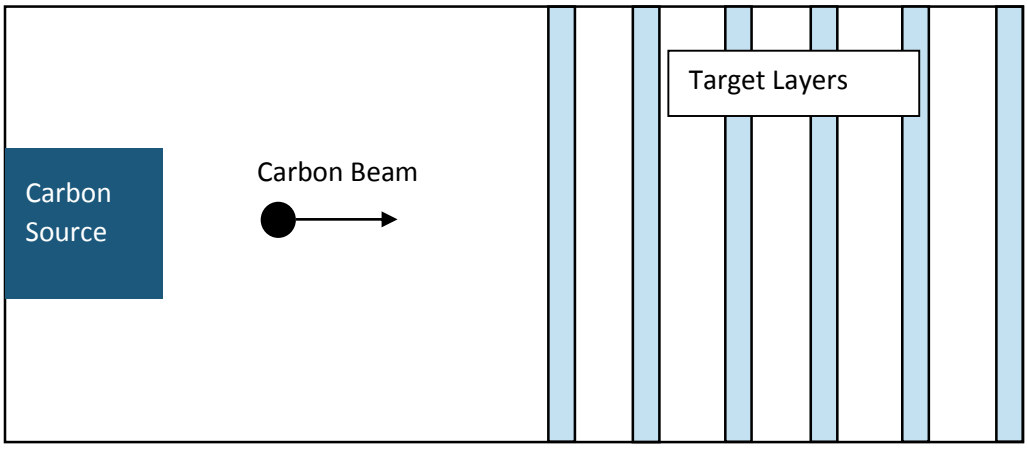

Figure 11: A schematic showing the target 'layers'. At each layer, the cross-section is integrated to determine the probability of interaction. If the projectile does interact, the probability of scattering towards the detector is found. If it does not interact, the projectile is advanced to the next layer. As soon as it has interacted, either towards the detector or not, the particle is discarded and a new projectile is considered.

As the projectile advances through the target layers, as shown in Figure 11, it will lose energy as it ionizes the target atoms. This energy loss is dependent upon the kinetic energy of the projectile, as well as its charge and mass. The magnitude of energy loss was found using the SRIM program [6], for both protons and deuterons. This data was loaded into the simulation and used to create a table of energy loss for various energies, which could then be interpolated between so as to obtain the energy loss for any desired energy. Once the projectile energy falls below 0.5 MeV, the simulation discards it, as it will no longer contribute scattered protons in the energy range of interest.

4.7 Simulation Runs and Usage

In this section the usage of the simulation program is outlined, followed by a description of the hardware used to run it. Finally, a table of parameters and their values for the simulation runs used to acquire data is presented.

4.7.1 Usage

The simulation was written in C++, using the Visual Studio 2012 IDE. As such it uses the Visual C++ compiler, and so the behavior of the simulation may be different and unexpected under different compilers.

There are 3 separate source files, each one dealing with a different aspect of the simulation – ^{12}C (d, p) ^{13}C, ^{12}C (d, d) ^{12}C, and ^{12}C (p, p) ^{12}C, where the first is the fusion reaction and the second two are the Rutherford scattering reactions. Each simulation has a 1000-layer-deep target, with energy loss tables calculated for the respective projectile. The simulations will run either until they have simulated 2E10 projectiles, or have counted a set number of successful scatters (for the results: either 100,200 or 300) towards the detector. To change the number of successes at which they finish, simply change the `proj_success` variable to the desired number.

Another variable, `bias_factor`, can be changed. This value, discussed earlier, will be multiplied by the probability of reaction at a layer, artificially increasing the probability of interaction. If set too high, the projectile will always react at the first layer it encounters, so it will have no opportunity to lose energy. If set too low, the simulation will take prohibitively long to run. The bias factors used to obtain the simulation data are included. The input energy can also be changed. This is the energy of the carbon beam being simulated. This can be set by the user, by changing the `initial_energy` variable. The angle of the detector relative to the beam can be set by modifying the `angle_of_interest` function.

To use the program, simply compile and run the source code using a C++ compiler – however, it is not guaranteed to operate as intended for compilers other than the Visual C++ compiler, as discussed above. The Fusion source code must be run in the same directory as the two text files containing the angular and energetic differential cross-sections discussed above. The results, 2 columns containing the scattering energy and angle of the resultant protons and deuterons, are output to a text file in the source code directory.

4.7.2 Hardware

The simulation was run using a Lenovo ThinkPad T430 laptop. This machine has a dual-core Intel i5-3210M CPU at 2.5GHz per core, 8GB of RAM, and runs Windows 7 Home Premium OS.

To run the fusion simulation and obtain a meaningful amount of data (a large number of successful scatters towards the detector), the simulation must simulate at least 1E10 projectiles, as the probability of interaction per layer is very low. A maximum bias factor of 10 can be used, as the probability of scattering towards the detector will be increased over 1 if a larger bias factor is used, forcing every particle to scatter towards the detector. An approximate time required to simulate a reaction, based on experience of running the simulations, is included in the simulation parameters table, Table 2.

4.7.3 Simulation Parameters

The simulation parameters for the simulations used for data acquisition are included below.

Table 2: Table of simulation parameters for the simulation runs used to acquire data.

Simulated Reaction	Beam Energy[MeV]	Bias Factor	Number of Successes	Simulation Time (Approx.)
^{12}C (d, p) ^{13}C	6.0	1E7	300	2 hours
^{12}C (d, d) ^{12}C	6.0	5,000	100	7 hours
^{12}C (p, p) ^{12}C	6.0	5,000	100	3 hours
^{12}C (d, p) ^{13}C	8.6	1E6	300	4 hours
^{12}C (d, d) ^{12}C	8.6	5,000	200	10 hours
^{12}C (p, p) ^{12}C	8.6	5,000	200	6 hours

4.7.4 Source Code

All source codes and required files can be downloaded using the following Google Drive link:

https://drive.google.com/folderview?id=0By_ODAJCH67USDZRazIzdk9jSXc&usp=sharing

5 RESULTS

Several simulations were run, using the parameters set out in Table 2. The results of these simulations, plotted using Excel, are shown below.

5.1 ^{12}C (p, p) ^{12}C RUTHERFORD SCATTERING

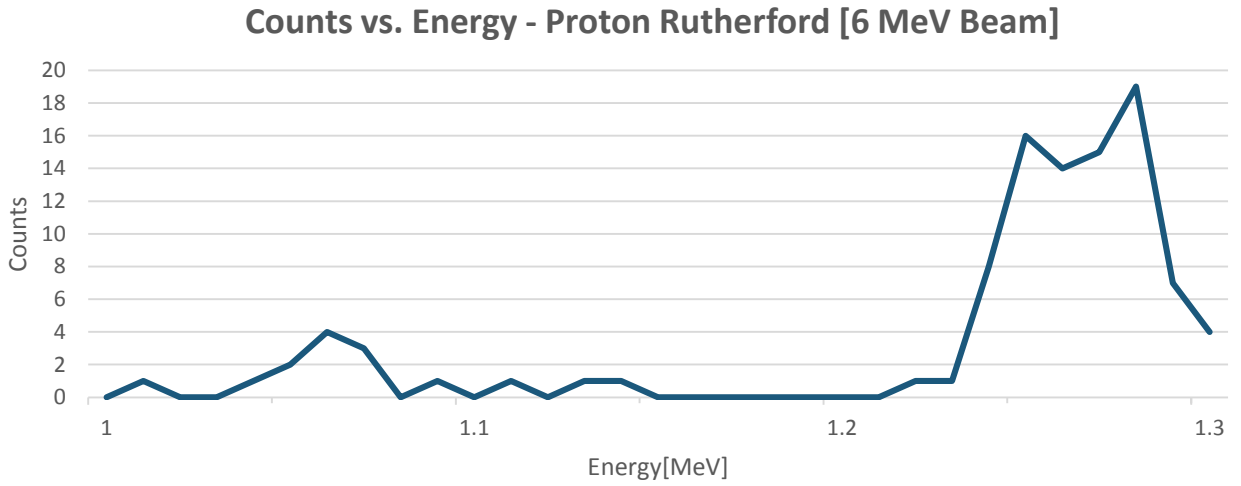

Figure 12: Results of the simulation for a 6 MeV carbon beam, scattering a proton in the target, which undergoes Rutherford scattering with a ^{12}C nucleus. (Detector Angle: 143˚, Number of Projectiles: 193,065, Number of Successes: 100).

Figure 12 shows the results of a simulation run, with bias factor 5,000 and carbon beam energy of 6 MeV aiming to simulate the ^{12}C (p, p) ^{12}C Rutherford scattering reaction. The peak of this spectrum, at approximately 1.27 MeV, is consistent with kinematic expectations for such a reaction.

The results for a simulation with identical parameters, except for a beam energy of 8.6 MeV, are much the same, as shown in Figure 13. The centre of the energy peak, approximately 1.8 MeV, is consistent with the kinematic predictions for such a reaction.

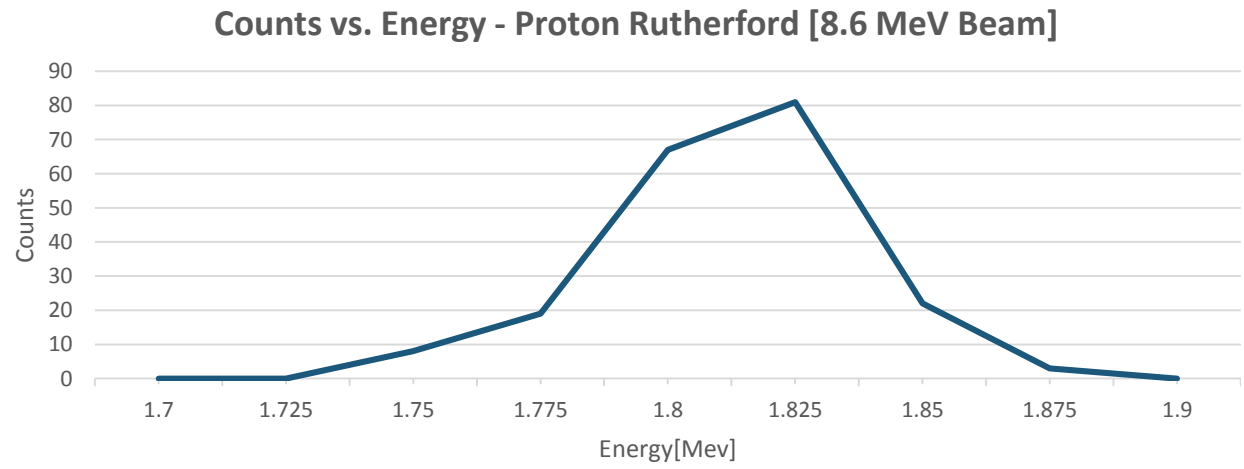

Figure 13: Results of the simulation for an 8.6 MeV carbon beam, scattering a proton inside the target. (Detector Angle: 143˚, Number of Projectiles: 325,597. Number of Successes: 200).

5.2 ^{12}C (D, D) ^{12}C RUTHERFORD SCATTERING

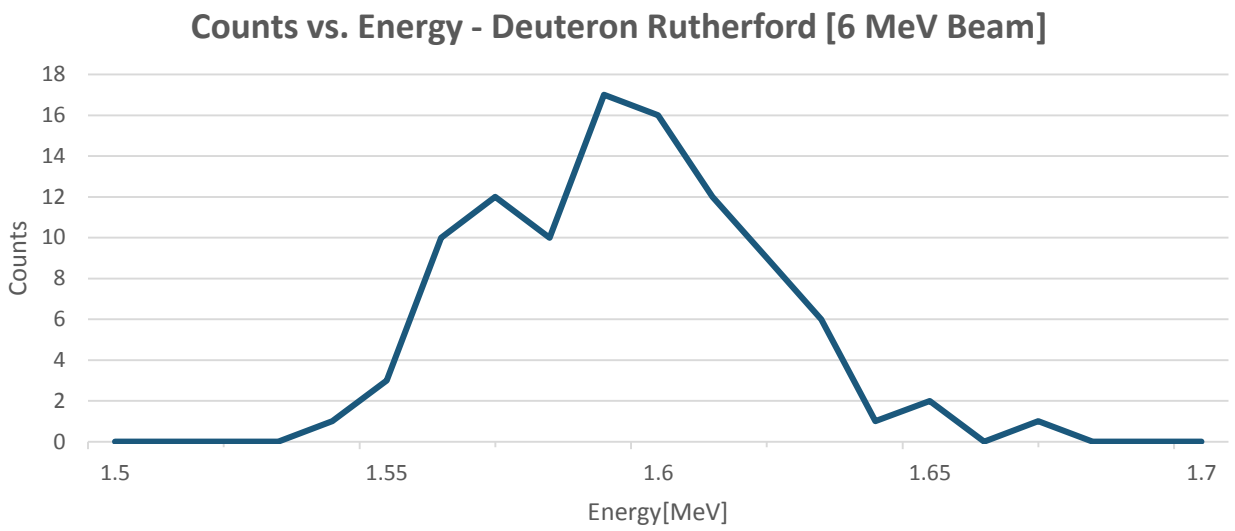

Figure 14: Results of the simulation for a 6 MeV carbon beam scattering a deuteron within the target, which undergoes Rutherford scattering with a ^{12}C nucleus. (Angle: 143˚, Number of Projectiles: 155,381, Number of Successes: 100).

Figure 14 shows the results of a simulation run with bias factor 5,000 and carbon beam energy of 6 MeV aiming to simulate the ^{12}C (d, d) ^{12}C Rutherford scattering reaction. The peak of this spectrum, at approximately 1.59 MeV, is consistent with kinematically expected energies for this reaction.

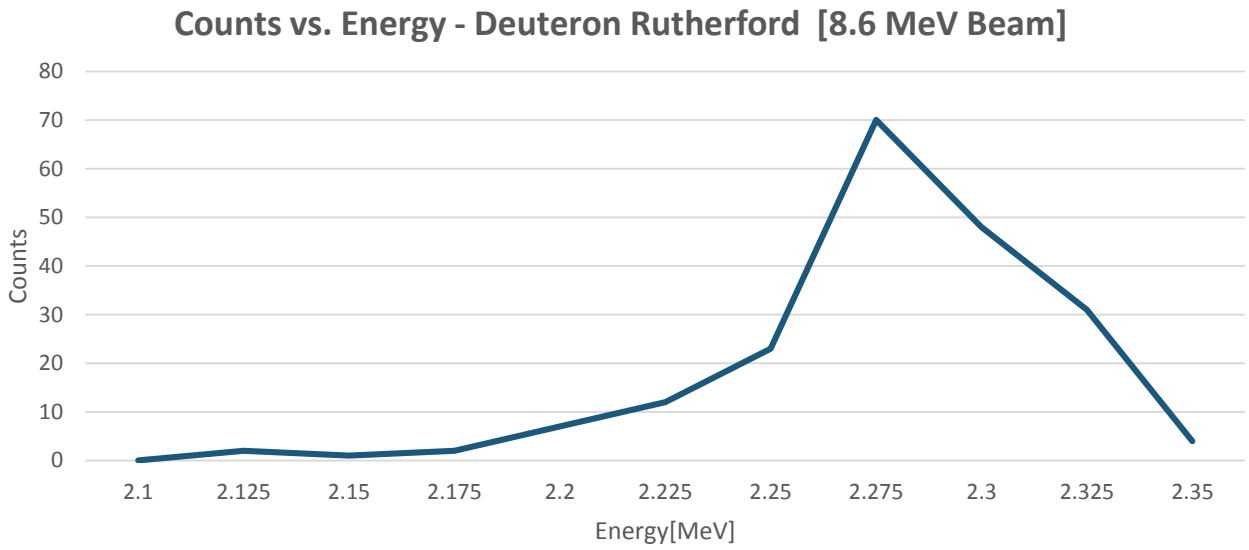

Figure 16: Results of the simulation for an 8.6 MeV carbon beam scattering a deuteron within the target, which undergoes Rutherford scattering with a 12C nucleus. (Angle: 143, Number of Projectiles: 379,195, Number of Successes: 200).

Figure 15 shows the results of a simulation run with bias factor 5,000 and carbon beam energy of 8.6 MeV. The peak of this spectrum, at approximately 2.27 MeV, is consistent with kinematically expected energies for this reaction.

5.3 ^{12}C (D, P) ^{13}C FUSION REACTION

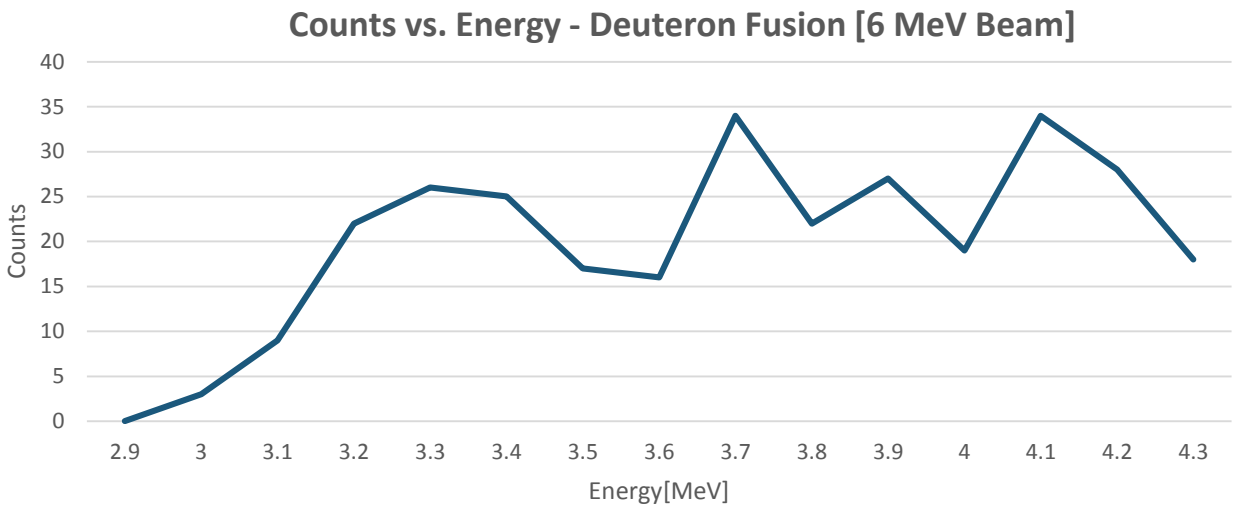

Figure 16: The results of the simulation run with carbon beam 6 MeV, scattering a deuteron in the target, which undergoes fusion with a ^{12}C nucleus. (Detector Angle: 143˚, Number of Projectiles: 488, Number of Successes: 200).

Figure 16 shows the results of a simulation run, bias factor 10, but with an additional bias factor of 1E7 that is not applied to the probability of scattering towards the detector, so as to increase the probability of interaction per layer. This does not change the angular or energy distribution of resultant particles, but will mean that each projectile will pass through a smaller average number of layers before interaction, and will therefore not lose so much energy due to ionization. This means that the simulation, although much quicker to run, will not be as accurate. This was done due to time constraints of the project.

The results show one interesting feature – a peak at 3.3 MeV, which is the kinematically expected energy of protons produced by fusion of 1.2 MeV deuterons with the carbon nucleus. This means that the fusion simulation can successfully simulate the fusion resonance at 1.2 MeV. The same 3.3 MeV peak can be seen in the simulation run for an 8.6 MeV carbon beam, in Figure 17.

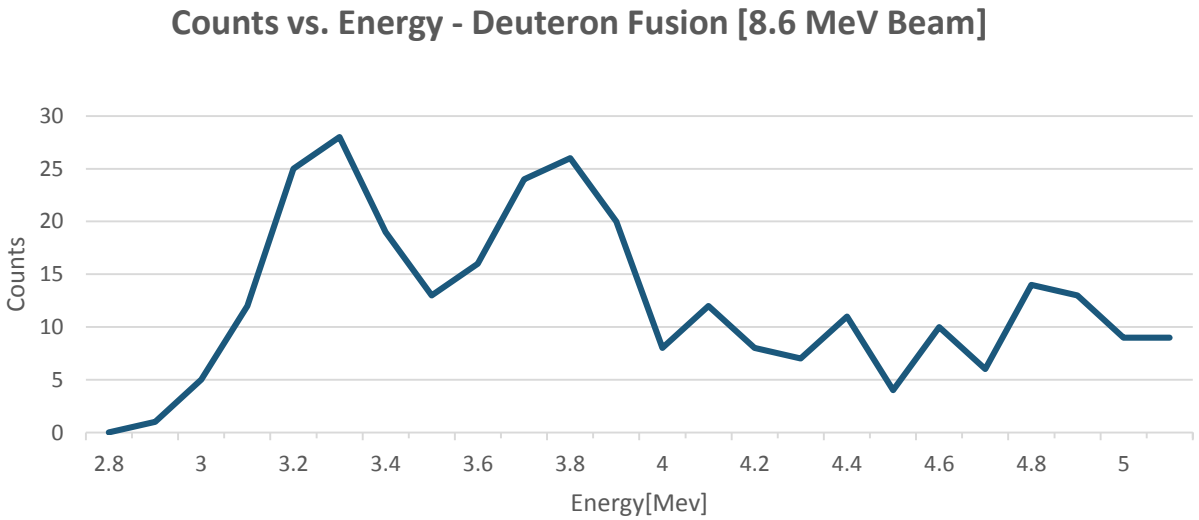

Figure 17: Results of the simulation run, bias factor 10, but with additional bias factor of 1E6. (Detector Angle: 143˚, Number of Projectiles: 1,918, Number of Successes: 200).

5.4 Comparison to Measured Data

In order to gauge the effectiveness of the simulation, the simulated data is compared directly to measured data. So as to visually compare the two, the simulated counts are scaled by an arbitrary factor so as to be directly comparable to the measured data.

5.4.1 6 MeV Carbon Beam

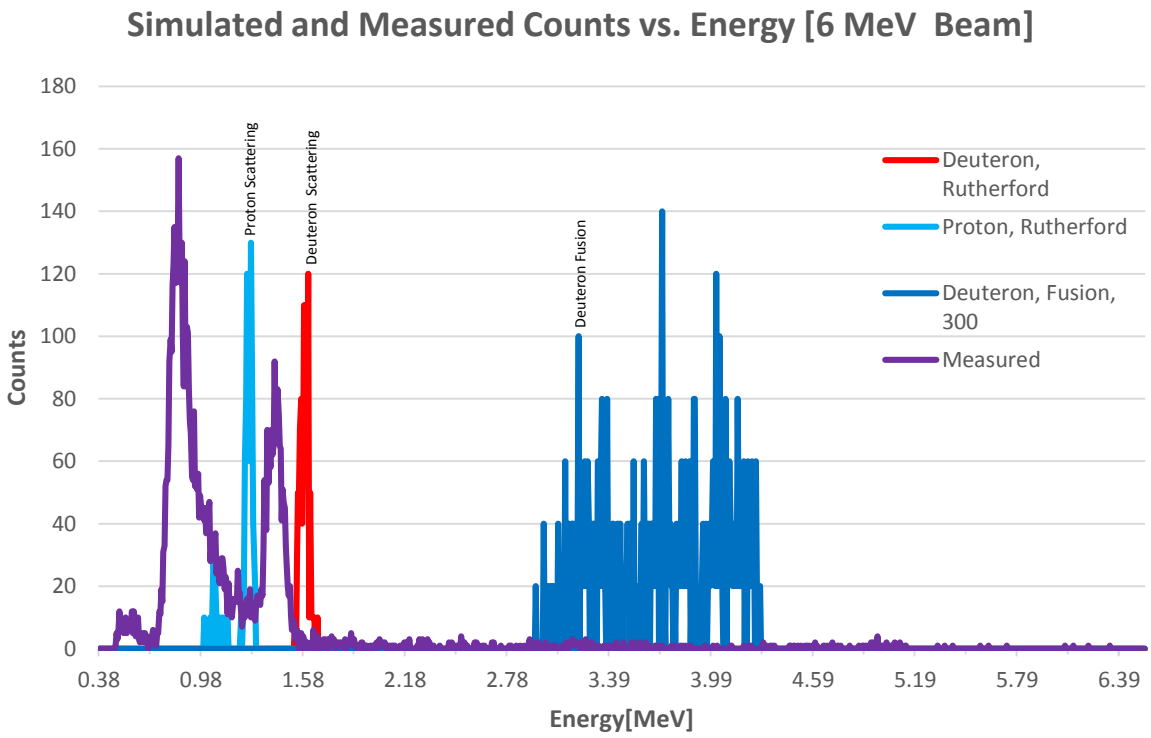

Figure 18: A comparison of the measured spectrum from a 6 MeV beam, and simulated data. The heights of the simulated data have been scaled to be comparable to the measured data.

Figure 18 shows measured counts compared with the simulated counts. Each simulation is scaled to be comparable in height to the measured data. Each peak has been labelled according to the 'primary' ejectile that is inducing the 'secondary' ejectile to be released.

The simulated ^{12}C (p, p) ^{12}C reaction appears to overlap with a measured peak, while the simulated position of the fusion peak is much greater in energy than any measured peak, suggesting that the fusion reaction contributes very little to the background at 6 MeV beam energy. However, this result is not reliable due to the additional biasing factor discussed above, which means that most of the simulated projectiles will not lose a significant amount of energy. If this additional bias was removed, then the projectiles would lose significantly more energy and the peak would be shifted to the left, towards lower energies.

The measured peaks contain both the desired carbon-fusion peaks, and the background radiation peaks from the two-step process. The overlap of the simulated two-step peaks, particularly the deuteron and proton Rutherford scattering peaks, suggests that the simulation will be useful in determining the energy of the background radiation peaks.

5.4.2 8.6 MeV Carbon Beam

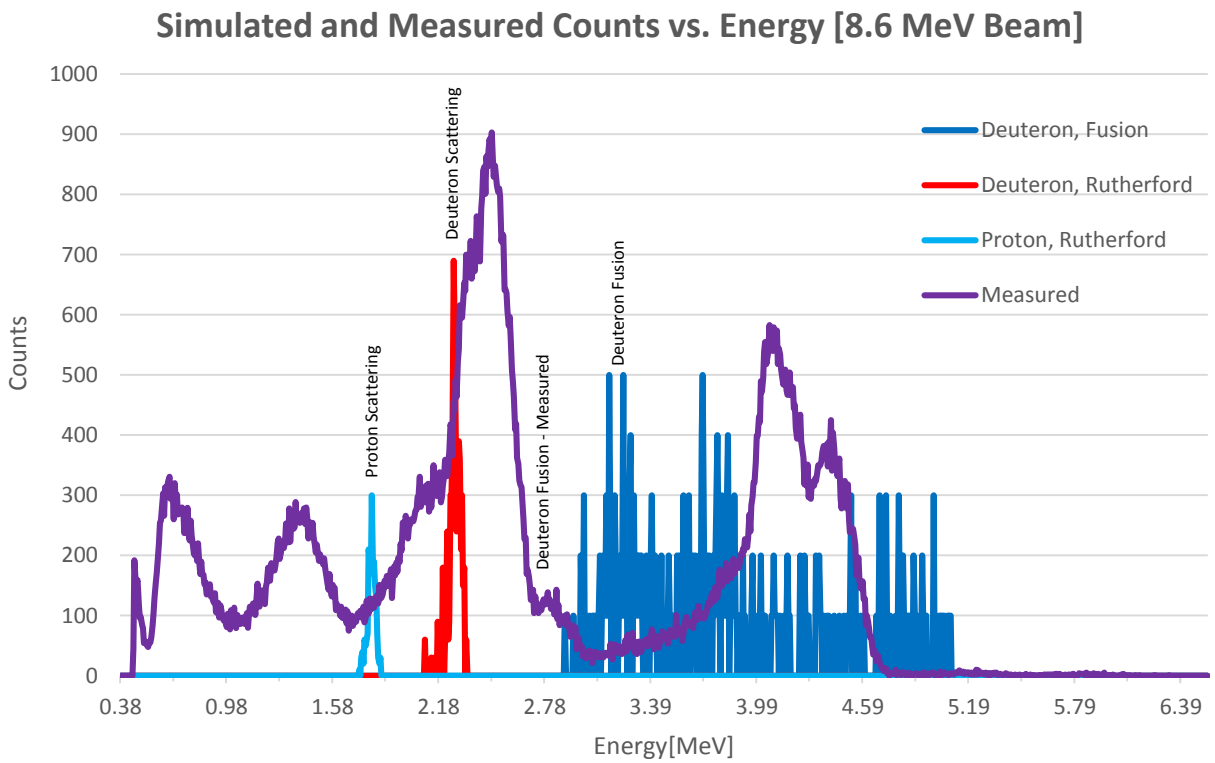

Figure 19: A comparison of the measured spectrum from an 8.6 MeV beam, and simulated data. The heights of the simulated data have been scaled to be comparable to the measured data.

Figure 19 shows measured data superimposed with the simulated counts. Each simulation peak is scaled to be comparable in height to the measured data. Each peak has been labelled according to the 'primary' ejectile that is inducing the 'secondary' ejectile to be released.

The simulated Rutherford scattering peak for deuterons appears to overlap with the measured 'lump' on the left of the largest measured peak. This suggests that the simulation results are accurate for Rutherford scattering of protons, while the Rutherford scattering peak for protons appears to be too great in energy – a rerun using a smaller bias factor so as to induce a greater energy loss may remove this discrepancy.

Finally, although the fusion simulation is not reliable, as discussed before, the simulated peak is close in energy to the measured peak. This suggests that the simulation is accurate in its modelling of the fusion reaction, and would be entirely accurate if the additional bias factor was removed.

5.5 Limitations of the Simulation

In order to make the simulation tractable, several approximations were introduced.

5.5.1 Worst Case Energy

After scattering by the ^{12}C beam, the 'primary' step ejectiles will have a range of energies, as shown in Figure 20.

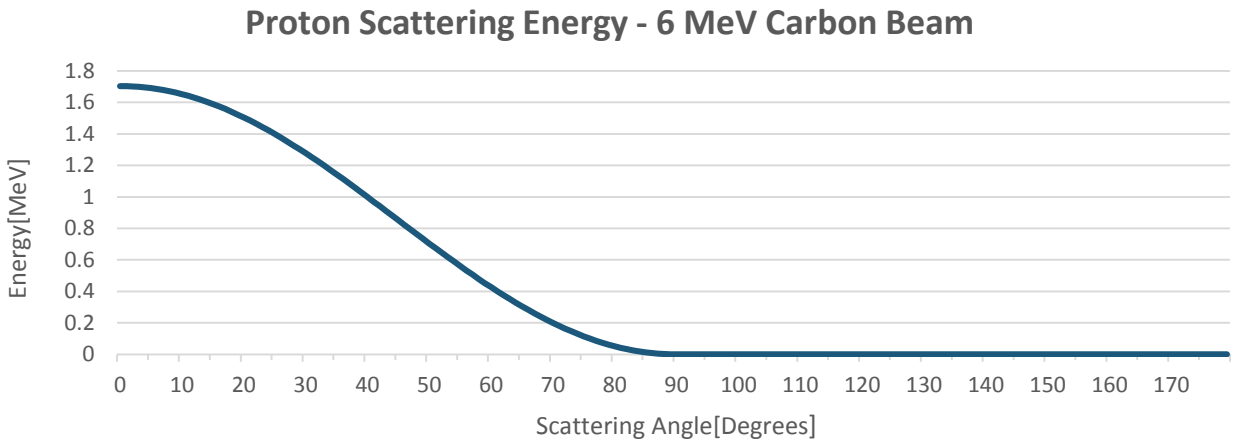

Figure 20: Proton energies after scattering by 6 MeV Carbon beam. Note the lack of protons scattered above 90˚ - there is no backscattering.

However, as the cross-section for Rutherford scattering increases significantly close to 0˚, there are far more protons scattered at low angles, close to 0˚, than at higher angles. Therefore, to simplify the code, every 'primary' step ejectile was considered to have been scattered at 0˚, and therefore had only the largest energy possible.

To improve the quality of the simulation, variation of the energy of the 'primary' ejectile could be introduced.

5.5.2 Output Resolution

The simulation will return both scattering angles and scattering energies for the 'secondary' step ejectiles. The energies are continuous, however, the scattering angles are in 1˚ increments. This will not hinder the use of the data produced, as the energy difference between 1˚ increments is smaller than the detector resolution.

5.5.3 Fusion Cross-Section

The method used to obtain an angular cross-section for a range of energies delivers only an approximation. However, this does not change the position of the energy peaks for the fusion simulation – only their shape, as the count rate will be different. To improve the simulation, a range of measured angular distribution for the cross-section for several energies must be found experimentally.

5.5.4 Fusion Over-Biasing

The extra bias factor for the fusion reaction discussed in the Results section is used to artificially increase the total probability of interaction per layer, so as to speed up the simulation. The probability per for scattering towards the detector, having interacted, is not multiplied by this extra bias factor, so the angular and energy distributions of scattered particles are not affected. However, as the particle will, on average, now pass through fewer layers before interaction, it will not lose as much energy through

ionization. Therefore, the increased bias factor will mean that the simulations results are not entirely representative of what will happen – although they can be used as a guide. To obtain more meaningful results, the extras bias factor must be removed – however, this will dramatically increase the length of time required to run the simulation before a substantial amount of data is collected.

6 CONCLUSION

In conclusion, the project has been successful in its aim of simulating the background radiation induced by the interaction of a ^{12}C beam with a carbon target. The carbon target had two main impurities, deuterium and hydrogen, which when subjected to the beam produced significant quantities of background radiation through a two-step process. This process was simulated using a C++ program that simulated the three main reaction channels, the ^{12}C (d, p) ^{13}C, ^{12}C (d, d) ^{12}C, and ^{12}C (p, p) ^{12}C reactions. In addition, the simulation has the capability of simulating energy loss due to ionization.

The results of the simulation, for both Rutherford scattering reactions, are consistent with kinematic expectations. For a beam energy of 8.6 MeV, where the positions of the measured background energies are clear, the simulated Rutherford peaks overlap with the observed peaks, suggesting that the simulation's results are valid.

For 6.0 MeV beam energy, the positions of the background peaks are less clear. The simulated Rutherford peaks overlap with the measured, allowing the energy of the background peaks within the measured spectrum to be determined.

In addition, the fusion reaction was simulated, with results consistent with kinematic expectations. The results also show a peak in proton production consistent with resonance for 1.2 MeV incident deuterons. These features are promising, but to obtain fully representative fusion results a much longer simulation run with no additional bias is required.

7 REFERENCES

[1] J. Zickefoose, J. Schweitzer and T. Spillane, "Low energy beam induced background studies for a 12C(12C, p) 23Na reaction cross section measurement," *Proceedings of Science,* 2010.

[2] P. Reichert, "3D-Hydrogen Analysis of Ferromagnetic Microstructures in Proton Irradiated Graphite," *Nuclear Instrumentation and Methods,* 2005.

[3] W. Jiang, "Carbon Analysis using Energetic Ion Beams," *Nuclear Instrumentation methods in Physics,* vol. 222, p. 538, 2004.

[4] G. Debras, "Light Elements Analysis and Application to Glass Industry," *Journal of Radioanalytical Chemistry,* vol. 38, p. 193, 1977.

[5] V. Zerkin, "Experimental Nuclear Reaction Data," EXFOR, 02 March 2016. [Online]. Available: https://www-nds.iaea.org/exfor/exfor.htm. [Accessed 15 March 2016].

[6] J. Ziegler, "SRIM - The Stopping and Range of Ions in Matter," 2009.

[7] M. Aliotta, *Private Communication,* 2016.

[8] L. Morales-Gallegos, M. Aliotta and et.al., "12C + 12C reactions at astrophysical energies: Tests of targets behaviour under beam bombardment," in *AIP Conference Proceedings*, Sicily, 2013.

[9] F. Strieder, "Laboratori Nazionali del Gran Sasso," 27 October 2009. [Online]. Available: http://npa4.lngs.infn.it/NPAIV_Contibutions/31d_Strieder.pdf. [Accessed 15 March 2016].

[10] C. Fonnebeck, A. Patil, D. Huard and J. Salvatier, "PyMC," 5 April 2012. [Online]. Available: http://pymcmc.readthedocs.org/en/jss-gp/theory.html. [Accessed 17 March 2016].